Modification of Active Sites on YSZ(111) by Yttria Segregation

Jayeeta Lahiri,[†] Adam Mayernick,[‡] Suzanne L. Morrow,[†] Bruce E. Koel,[§] Adri C. T. van Duin,[||] Michael J. Janik,[‡] and Matthias Batzill*,[†]

Department of Physics, University of South Florida, Tampa, Florida 33620, Department of Chemical Engineering, Penn State University, University Park, Pennsylvania 16802, Department of Chemistry, Lehigh University, Bethlehem, Pennsylvania 18015, and Department of Mechanical and Nuclear Engineering, Penn State University, University Park, Pennsylvania 16802

Received: November 19, 2009; Revised Manuscript Received: January 15, 2010

The surface properties of YSZ (111) have been investigated by X-ray photoemission spectroscopy (XPS), scanning tunneling microscopy (STM), temperature programmed desorption (TPD) of adsorbed formate, and computational studies using the ReaxFF reactive force field approach. XPS and computer simulations showed enrichment of the surface with yttria. STM studies indicated that a high density of step edges are readily formed with ∼35% of the surface sites located at steps. Step edges are identified as the primary adsorption sites for formate. The formate oxidizes in a dehydration reaction producing carbon monoxide and water at ∼600 K. This is contrasted to the reaction of formate on pure zirconia where formate reacts by both dehydration and dehydrogenation reactions. This shift in the selectivity between pure zirconia and yttria-doped zirconia is attributed to the modification of the active step edge sites by yttria segregation. Therefore, the modification of active sites by minority species in a mixed oxide can control the chemical surface functionality.

1. Introduction

Mixed oxide ceramics, i.e., solid solutions or alloys of two or more oxides, are an important class of functional materials, where the second component (additive) can strongly affect mechanical[1] and chemical properties. The chemical surface properties of these ceramics depend on their surface composition and structure. Segregation of minority components may alter the surface properties and consequently allow tuning of the chemical functionality of the material. Here we examine the surface properties of yttria-doped zirconia as a model system for mixed oxide catalysts.

Yttria-stabilized zirconia (YSZ) is a solid-solution ternary system with an yttrium-to-zirconium ratio typically around 1:9. Yttria is added to zirconia to stabilize zirconia's cubic high temperature phase. Furthermore, the difference in the valency of Y(III) and Zr(IV) results in a high density of unoccupied anion sites in the fluorite structure of zirconia. This is the underlying reason for the high oxygen-ion conductivity of YSZ that was discovered already by Nernst more than 100 years ago,[2] and is exploited today for oxygen sensors and in membranes for solid oxide fuel cells. Other prominent applications of YSZ are as heat barrier coatings for turbine and jet engine blades[3] and as heterogeneous catalyst and catalyst support material.[4] YSZ is a potential catalyst, with superior stability compared to noble metal catalysts, for the partial oxidation of methane to synthesis gas. YSZ is a more active catalyst than its components, i.e., pure ZrO_2 or Y_2O_3.[5] In order to fundamentally understand this special activity of the mixed oxide, we use surface science techniques in ultrahigh vacuum (UHV). We investigate the reaction of formate by temperature programmed desorption (TPD) on YSZ and compare it with reactions on thin films of pure zirconia and yttria grown on the YSZ substrate.

Formate is an important reaction intermediate in the water−as shift reaction of metal oxides and the partial oxidation of methane to synthesis gas. It is also a common probe molecule to characterize the base/acid properties of oxides in TPD studies.[6] Typically, dehydration reactions of adsorbed formate, formed by dissociative adsorption of formic acid, ($HCOO^* + H^* \rightarrow CO + H_2O$) occurs on acidic oxides, while dehydrogenation ($HCOO^* + H^* \rightarrow CO_2 + H_2$) is observed on basic oxides. Contrary to this assessment, single-crystal UHV studies have observed dehydration reactions on basic MgO(100)[7] and CeO_2(110)[89] surfaces. This implies that the reducibility of the substrate is equally important for the dehydrogenation reaction and that lattice oxygen is directly involved in forming CO_2 reaction products.[10,11]

Previous experimental[12,13,5] and theoretical[14,15] investigations on the surface composition of YSZ-ceramics suggest yttrium enrichment compared to the bulk. Surface segregation is a common phenomenon in multicomponent materials and can dramatically influence the functionalities of materials.[161] Segregation can, for instance, cause the formation of highly active sites for surface reactions. In studies of partial methane oxidation to synthesis gas over YSZ catalysts, Zhu et al. reported that the yttrium doping of zirconia improves the catalytic performance significantly compared to pure zirconia due to the formation of more active sites.[5] On YSZ, methane was activated to formate at the surface, which then decomposed to an almost equimolar mixture of CO, CO_2, H_2 and H_2O.[4] The activity of YSZ increased with increasing calcination temperatures. This was associated with the exposure of low index planes,[17] in particular the (111) face, which exhibits the lowest surface energy for YSZ.[15] Previous studies on YSZ catalysts thus illustrate that yttria in the surface layer strongly affects the surface chemical properties.

* Corresponding author. E-mail: mbatzill@cas.usf.edu.
[†] University of South Florida.
[‡] Department of Chemical Engineering, Penn State University.
[§] Lehigh University.
[||] Department of Mechanical and Nuclear Engineering, Penn State University.

10.1021/jp9109964
Published on Web 03/08/2010

The complexity of "real" catalyst materials makes a conclusive interpretation between structure/composition and chemical properties difficult. Thus we use simplified single-crystal model systems in connection with atomistic computations to unravel the synergy between segregation behavior and surface chemical reactivity of YSZ. There are only a few reports of surface science studies that have attempted to investigate the role that different components in mixed oxides play in determining the surface chemical properties.[18] Here we show that step-edges are important active sites on YSZ and that yttrium segregation to step edges shifts the selectivity of formate oxidation from dehydration to dehydrogenation compared to pure ZrO_2. Computational results using density functional theory (DFT) and reactive force-field (ReaxFF) methods are used to corroborate the segregation of Y to the surface and step edge sites.

2. Methods

To understand the synergies between surface composition and structure and the chemical surface properties of complex mixed oxide materials, we employed a combination of UHV surface science studies and advanced computational modeling. In the following two subsections, we briefly describe the experimental and theoretical methods.

2.1. Experiment. Epi-polished single-crystal YSZ(111) samples were obtained from MTI Corporation. The samples were cleaned by sonication in acetone, ethanol, and deionized (DI) water. Another set of samples was additionally annealed in a tube furnace to 1300 K in atmospheric pressure O_2 prior to introduction into the vacuum chamber. The scanning tunneling microscopy (STM) measurements and TPD studies were performed in two different UHV chambers. In the STM chamber, the samples were heated by an indirect resistive heating plate to 1000 K in 10^{-6} Torr O_2. The sample temperature during annealing was calibrated by a thermocouple directly attached to the surface of a YSZ plate with a ceramic adhesive (Aremco 835). The samples were then investigated by high-temperature STM at a sample temperature of around 550 K using an Omicrometer VT-STM. At lower temperatures, the ion conductivity was too low for STM measurements to be made.[19] Samples treated by the two ex-situ prepreparation methods differed in the large scale step edge morphology, as has been reported previously.[20] The terrace structure did, however, exhibit similar nanoscopic monolayer deep holes. Samples were cleaned in situ by ion sputtering with 0.8 keV Ar^+ ions at an elevated sample temperature of 600 K. The elevated temperature avoids surface charging and ensures that preferential sputtering of oxygen is compensated by oxygen diffusion from the bulk. After sputtering, samples were annealed in situ in 10^{-6} Torr O_2 at 1000 K prior to STM imaging.

In order to determine the surface composition, we employed high-resolution X-ray photoemission spectroscopy (XPS) at the Scienta ESCA-300 system at Lehigh University. Samples from the same batch used for the other experiments were examined by angle-resolved photoemission studies. The Y-3d and Zr-3d peaks were monitored as a function of polar emission angle. These polar scans were taken at a random azimuthal orientation with 5° steps from normal emission to 75°.

TPD studies were performed in a separate UHV chamber. Sample preparation was similar to those in the STM chamber. The samples were mounted on a Ta-plate that was heated resistively with a constant heating rate of 1 K/s, and the temperature was monitored by a thermocouple directly attached to the surface of the YSZ sample by a ceramic adhesive. Formic acid was dosed with a direct gas doser with the sample at room

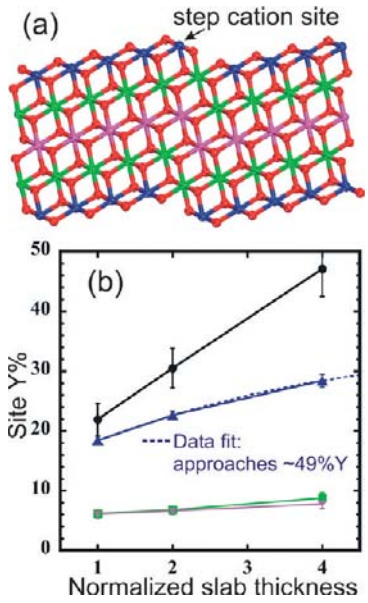

Figure 1. (a) Thinnest ReaxFF slab model of the YSZ surface with blue atoms corresponding to surface metal atoms, green atoms as second layer metal atoms, purple atoms as third layer metal atoms and red atoms as oxygen. (b) Y% at the step edge (●), surface (■), second surface layer (▼), and third surface layer (▲) on the YSZ surface as a function of slab thickness.

temperature. All samples discussed here were exposed to ~1 L (Langmuir) formic acid measured with an ion gauge in the vacuum chamber without taking doser enhancement factors or ion gauge sensitivity factors into account. The dose corresponded to a saturation dose, i.e., larger doses did not cause increases in the desorption peaks. The desorption products were monitored with a UTI quadrupole mass spectrometer. CO, CO_2, and H_2O were monitored because these are the reaction products for oxidation of formate. Formic acid desorption was also monitored, but no desorption signal was detected. Prior to every dose, the samples were annealed in 10^{-6} Torr O_2 for 30 min at 700 K and subsequently in UHV for 10 min at the same temperature.

Ultrathin films of pure ZrO_2 or Y_2O_3 were grown by reactive molecular beam epitaxy (MBE). Zr or Y was evaporated from a solid rod by a mini e-beam evaporator in 10^{-6} Torr O_2 background pressure and a sample temperature of 600 K. The deposition rate was ~0.1−0.2 nm/min calibrated by a quartz microbalance. The total film thickness was ~3 nm. In-situ XPS was used to verify that the Y or Zr signal was suppressed to ensure a pure ZrO_2 or Y_2O_3 surface termination, respectively.

2.2. Computer Simulation. Simulations were performed using the ReaxFF Monte Carlo Reactive Dynamics Method[21] to sample possible surface configurations of yttrium atoms and oxygen vacancies and locate minimum energy geometries. DFT calculations were used to reparameterize the ReaxFF force field to accurately model the YSZ (111) surface. Figure 1a displays the surface model used in our ReaxFF Monte Carlo simulations. The stepped YSZ (111) surface was modeled by vicinal surface slabs of termination (10 10 8), with one step on each side of the slab. Simulations were performed using different slab thicknesses to investigate the dependence of yttrium surface segregation on the YSZ bulk:surface ratio. Figure 1a represents the thinnest slab used. A detailed description of the DFT and ReaxFF methodology and results is given elsewhere.[22]

3. Results

3.1. Surface Composition of YSZ(111). High-resolution XPS shows that the as-received samples have small amounts

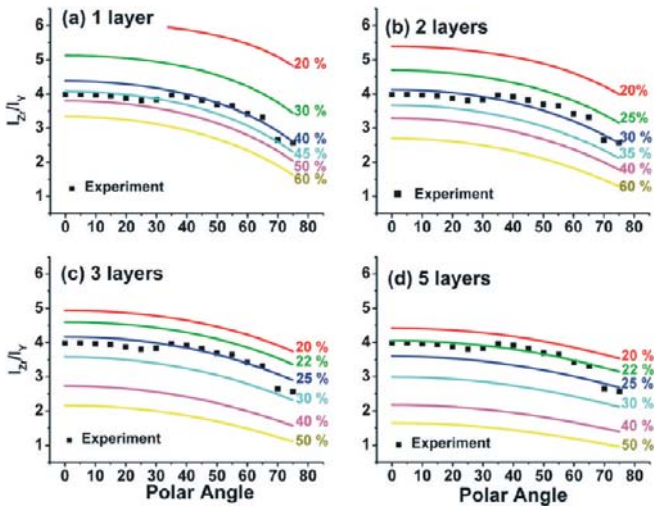

Figure 2. Polar-angle-dependent photoemission intensity ratio of Zr-3d and Y-3d peaks for experiments (black squares) and calculated intensity ratios for a two-layer model. Different Y-enriched surface layer thicknesses are considered with one monolayer (a), two monolayers (b), three monolayers (c), and five monolayers (d). The bulk composition was kept at 90% Zr and 10% Y, while the surface composition was varied from 20 to 60% yttrium. From the match of the intensity ratio and angle dependence, we deduce that the surface layer is best described by a one or two monolayer-enriched region with a 45% or 30% Y concentration, respectively.

of surface contaminations, such as Si and P. Also, angle-dependent XPS studies show an enrichment of the surface with yttrium. Figure 2 shows the variation of the peak intensities of Zr-3d/Y-3d as a function of takeoff angle for a random azimuthal crystal orientation. As the emission angle increases, the relative intensity of the Y-3d peak relative to the Zr-3d peak increases and thus the Zr/Y intensity ratio decreases. This indicates that the surface layer is Y-enriched because at larger emission angles XPS becomes more surface sensitive. The Zr/Y ratio does not decrease uniformly with increasing emission angle, but instead peaks at ~40°−60° are observed. These variations are due to photoelectron diffraction effects on the single crystal sample. These variations are very pronounced for the intensities of the individual elements. One may expect that Zr-3d and Y-3d show very similar photoelectron diffraction effects because of the same symmetry of the electronic state and because Zr and Y occupy the same lattice sites in YSZ. Consequently, the photoelectron diffraction effects are suppressed noticeably in the ratio of the intensities. Nevertheless, residual fluctuation is observable mostly because of the composition variation in the surface layer.

If we neglect the photoelectron diffraction effects, we can estimate the surface enrichment of YSZ with yttrium. The variation of the intensity ratio as a function of polar angle can be compare with the theoretical intensity ratio for a model system consisting of a Y-enriched surface layer and a bulk with a Zr/Y ratio of 9:1. Such a stratified model is a simplification and does not take into account a more realistic gradual concentration variation. Nevertheless, it provides a reasonable estimate for the surface enrichment, in particular if the enriched layer is very thin, and it becomes an accurate model if only the topmost layer is enriched. The advantage of this model is that we have only two parameters, i.e., the surface layer composition and the thickness of the surface layer. Estimating the inelastic mean free path of photoelectrons according to the method of Seah and Dench[23] for the Zr-3d and Y-3d lines gives values of $\lambda_{Zr} = 4.28$ nm and $\lambda_Y = 4.31$ nm, respectively, which are close to the values expected from the "universal curve" for photoemission. Atomic sensitivity factors for Zr-3d ($A_{Zr\text{-}3d} = 2.1$) and Y-3d ($A_{Y\text{-}3d} = 1.76$) were taken from ref 24. Using these values, we can write the peak ratios by the following expression for the two layer model:

$$\frac{I_{Zr}}{I_Y} = \left(\frac{A_Y}{A_{Zr}}\right) \times \left[\frac{C_{Zr,s}\sum_{i=0}^{n} \exp(-id/\lambda_{Zr}\cos\theta) + C_{Zr}\int_{(n+1)d}^{\infty} \exp(-z/\lambda_{Zr}\cos\theta)\mathrm{d}z}{C_{Y,s}\sum_{i=0}^{n} \exp(-id/\lambda_{Y}\cos\theta) + C_{Y}\int_{(n+1)d}^{\infty} \exp(-z/\lambda_{Y}\cos\theta)\mathrm{d}z}\right]$$

Here the summation is over the number of surface layers n with every layer having a separation of $d = 0.3$ nm, i.e., the interlayer separation between (111) planes. The bulk contribution has been evaluated by integration of the intensity from the first bulk layer, i.e., $(n + 1)$, to infinity. The surface-layers have a yttrium composition of $c_{Y,s}$ (the surface zirconium concentration is $c_{Zr,s} = 1 - c_{Y,s}$, accordingly), and the bulk was kept constant at $c_Y = 0.1$ and $c_{Zr} = 0.9$. Calculated results for $n = 1$, 2, 3, and 5 and various surface concentrations for yttrium are shown in Figure 2a−d, respectively together with the measured intensity ratios. First, we consider normal emission only, i.e., $\theta = 0$. If there was not any surface enrichment in yttrium, i.e., the sample was uniform, we would expect a ratio of $I_{Zr}/I_Y = 7.5$. The experimental value of $I_{Zr}/I_Y = 4$ thus indicates a Y-enrichment in the surface layer. Depending on how many layers (n) are enriched, we fit the experimental value to a surface concentration of yttrium of $c_{y,s} = 45\%$, 30%, 25%, or 22% for $n = 1$, 2, 3, or 5, respectively. This leaves us with the questions of how many of the surface layers are in fact Y-enriched. By investigating the variation of the I_{Zr}/I_Y as a function of angle, we find that only for $n = 1$ or 2 is the experimental angle dependence reproduced satisfactorily. For thicker enriched surface layers, the variation as a function of polar angle is less strong. This visual inspection is confirmed by calculating the agreement between experimental values and expected intensity ratios from the layer model. Using the r^2 method, the reliability values can be calculated as follows:

$$r^2 = 1 - \frac{\sum_i (Y_i^{Cal} - Y_i^{Exp})^2}{\sum_i (Y_i^{Cal} - \overline{Y^{Exp}})^2}$$

We obtain values of 0.95, 0.98, 0.84, and 0.45 for $n = 1$, 2, 3, and 5, respectively, indicating that the best agreement between experiment and the layer model is achieved for $n = 1$ and 2. Therefore, we conclude that the surface has a Y concentration between 30−45%, and the enrichment is either only in the first or the first two layers. The ReaxFF simulations discussed below support enrichment in the topmost surface layer only, with a slightly higher enrichment (~49%) than deduced from the XPS measurements.

3.2. Surface Morphologies. The insulating character of many bulk oxide surfaces makes a determination of the nanoscale surface structure challenging. Recently we reported that the high ion mobility in YSZ enables STM characterization of YSZ at elevated temperatures.[19] Although detailed atomic scale information has not yet been achieved, important information of the nanoscale defect structure is obtained. Figure 3 shows the

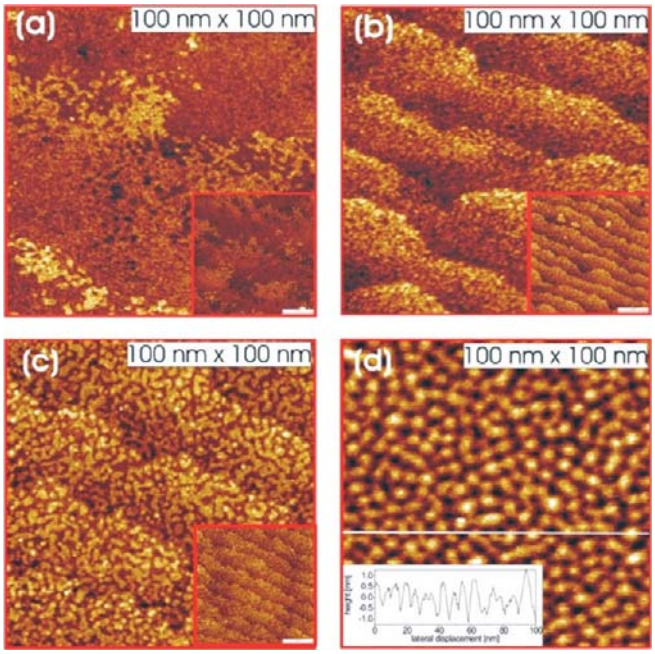

Figure 3. STM images of YSZ(111) surfaces as-received (a), annealed in atmospheric pressure O_2 at 1000 °C (b), sputtered and annealed in UHV at 800 °C (c), and after many sputter and annealing cycles (d). The STM images are 100 × 100 nm^2; the insets in panels a, b, and c are 200 × 200 nm^2. In c, the surface is covered with a high density of monatomic height "islands" superimposed on the large scale step-edge morphology. Therefore, this surface exhibits an extremely high density of step-edges. The inset in d shows a line-scan indicating the crest-to-valley corrugation is 1−2 nm, and thus indicating a high step edge density.

surface morphologies of differently prepared YSZ(111) samples. In Figure 3a, an STM image of an "as received" epi-polished YSZ substrate is shown. The only sample treatment was by annealing at ∼900 K in a 10^{-6} Torr O_2 atmosphere in order to "burn off" any carbon from the surface. These epi-polished surfaces are very flat with terraces on the order of 10−40 nm wide. The terraces are separated by step edges that appear "fragmented", i.e., the change from one terrace to another extends over some width that consists of meandering step edges and isolated monatomic height islands. This "fragmented" step edge morphology does not change even after extended annealing at 900−1200 K in vacuum. Annealing to higher temperatures caused a reduction of the samples, indicated by a discoloration of the crystal due to formation of color centers. Such reduced samples can no longer be imaged by STM, presumably because of a lack of mobile oxygen ions.

Figure 3b shows an STM image of a sample annealed in a tube furnace in atmospheric pressure O_2 prior to introduction into the UHV chamber. Such samples exhibit "compact" step edges, i.e., the change from one atomic-layer to the next occurs at a single step. Thus, annealing in oxygen at atmospheric pressure apparently results in a larger mobility of surface atoms and consequently in a surface smoothing. This contrasts to vacuum annealing, where a rearrangement of surface atoms is obviously hindered.

After 0.8 keV Ar^+ sputtering and annealing, the surface exhibits a large density of step edges. Figure 3c shows the surface after sputtering and vacuum annealing to 1000 K, and Figure 3d shows the surface after prolonged sputtering with an ion fluence of 7 × 10^{16} ions/cm^2 and vacuum annealing at 1000 K. Similar surface morphologies are obtained after repeated sputtering cycles. The surface roughens with increasing sputtering, and even high temperature annealing in vacuum or low O_2 pressures does not reform a flat surface. This is consistent with our observations of the "as-received" samples for which the step edge structure was also not affected by vacuum annealing. The step-edge density can be measured from Figure 3c. An analysis of this and similar images gives a total step length of ∼8400 nm in a 100 × 100 nm^2 area. Using a cation density on the YSZ(111) surface of 8.78 cations/nm^2 and a line density of 2.76 cations/nm for step edges along the densely packed ⟨110⟩ direction, we find that ∼35% of all surface atoms are located at step edges on this surface. This high density of special sites has a strong impact on the surface chemical properties, demonstrating the importance of real space surface imaging.

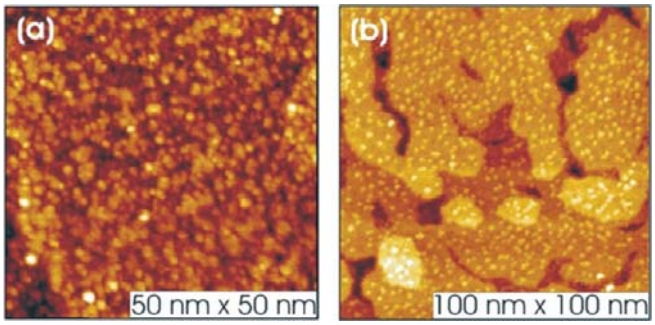

Figure 4. STM images of ZrO_2 film grown on YSZ(111). The as-grown film shown in panel a has a large density of monatomic height step edges. After annealing in atmospheric pressure O_2, the surface exhibits large terraces as shown in panel b. The origin and composition of the "bright spots" on these terraces is unknown.

In order to compare the surface properties of YSZ with those of pure Y_2O_3 or ZrO_2, thin films of zirconia or yttria were grown on the YSZ substrates by reactive MBE. These samples are very difficult to measure with STM because of their excellent insulating properties. Nevertheless, we succeeded in measuring ∼2 nm thin ZrO_2 films grown at 300 °C. This sample exhibited a rough surface with a high density of step edges. An STM image of the surface is shown in Figure 4a. Annealing the sample in a tube furnace reduced the step density, as is evident from Figure 4b. No measurements on Y_2O_3 thin films could be performed because of their insulating properties.

3.3. Computation of Y-Segregation Behavior. XPS measurements showed a strong yttrium enrichment of YSZ(111), and STM studies revealed the formation of stepped surfaces by vacuum preparation. In order to study whether step-edges and flat (111) terraces exhibit different Y-enrichment at the surface, ReaxFF computation was employed.

ReaxFF calculations were performed for different slab thicknesses. The thinnest slab considered is shown in Figure 1a, and the maximum slab thickness was 4 times the slab shown in Figure 1a. Thicker slab sizes were not considered due to prohibitive computational requirements of performing such simulations. For all the slabs considered, an enrichment of the surface with Y was observed, indicating that it is thermodynamically favorable for yttrium atoms to segregate to the surface of YSZ(111). In addition, the step edge exhibited an even higher Y concentration than the terraces. Figure 1b summarizes the computed Y-segregation as a function of slab thickness. This plot shows the percentage of metal sites occupied by yttrium for the step edge, surface, and subsurface layers of YSZ with 10% yttrium. The increase of Y-segregation with slab thickness is a consequence of the increased bulk-to-surface ratio, which gives a larger "Y-reservoir" for thicker slabs. Therefore, in order to compare these computations to the experimental system for

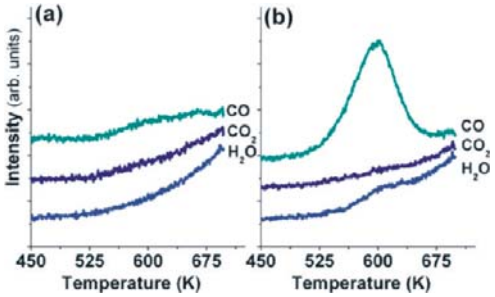

Figure 5. TPD traces for CO, CO_2, and water from formic acid adsorbed at room temperature on YSZ(111) for as-received samples (a) and after sputtering and annealing in UHV (b).

which the bulk concentration is effectively not affected by surface segregation, the computational results should be extrapolated to infinite thickness. The Y concentration at terrace increases with slab thickness but appears to start to saturate with increasing slab thickness. Using a second-order polynomial to fit the data points suggests a saturation of Y-enrichment at around 49%, which is in surprisingly good agreement with the XPS results discussed above. The enrichment at the step edge, on the other hand, does not appear to saturate with film thickness, implying that the step edges become completely yttria terminated for a large enough yttrium reservoir in the system. Furthermore, the simulations show that yttrium enrichment occurs in the surface layer of YSZ only, and no enrichments in the second or third layer are observed in our limited slab thicknesses, in further agreement with the XPS analysis.

The result that step edges on YSZ are mainly yttria terminated should have implications for the chemical activity of the prepared surfaces since undercoordinated step-edge sites are often associated with active sites on oxide surfaces. To probe this surface chemistry, formate reaction at differently prepared surfaces was investigated, which is discussed next.

3.4. Formate Temperature Programmed Desorption. TPD studies of formate formed by dissociative adsorption of formic acid were carried out on YSZ(111) substrates and pure ZrO_2 and Y_2O_3 thin films. TPD spectra were measured for differently prepared samples. We observe weak CO and sometimes CO_2 desorption signals at 400 K for all samples. This is attributed to desorption from the sample mount and are not considered any further. The main desorption signal was observed at around 600 K, which is consistent with formic acid oxidation temperatures on other metal oxide surfaces.[25] Hydrogen and water are expected as reaction products for dehydrogenation and dehydration reactions, respectively. Some small water desorption peak is observed together with CO for dehydration reactions; however, the intensity ratio of CO to water is much larger than expected. Also, we were not able to detect H_2 for any reactions. Therefore it seems likely that hydrogen diffuses into the bulk or desorbs at much higher temperatures. Our observations of smaller than expected water and hydrogen signals has also been observed by others for formic acid reactions on metal oxide surfaces, such as YSZ(100)[26] and TiO_2(001).[27] Therefore we concentrate on the CO and CO_2 signals for description of the surface reactions.

The TPD spectra for YSZ are shown in Figure 5. For "as-received" samples or samples that have been annealed in a tube furnace, very little desorption products were observed after "cleaning" in UHV by annealing in 10^{-6} Torr O_2. This indicates that formic acid does not adsorb on these surfaces at room temperature. The TPD spectra change dramatically after sputtering and annealing, i.e., a procedure that STM images showed

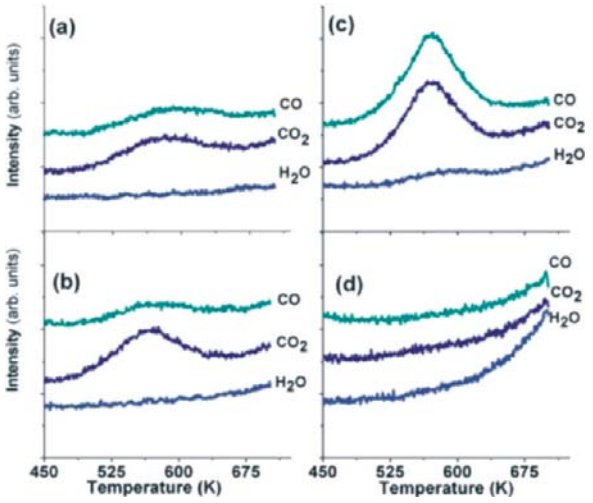

Figure 6. TPD traces for CO, CO_2, and water from formic acid adsorbed at room temperature on ZrO_2 films grown on YSZ(111) samples for as-grown samples (a), after annealing in 10^{-6} Torr O_2 (b), after sputtering and annealing in UHV (c), and after annealing ex situ in atmospheric pressure O_2 at 1000 °C.

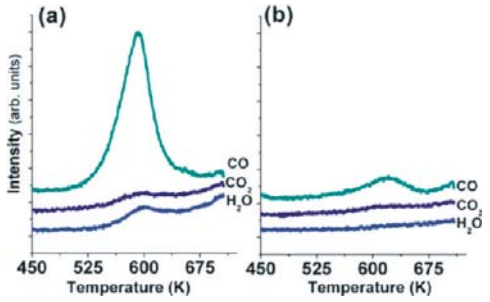

Figure 7. TPD traces for CO, CO_2, and water from formic acid adsorbed on Y_2O_3 films grown on YSZ(111) for as-grown samples (a) and after annealing of the sample in atmospheric pressure O_2 at 1000 °C (b).

to produce a high density of step edges. After this sample preparation, a strong CO desorption peak together with H_2O desorption is observed at 600 K. The same desorption temperature for water and CO indicates that the desorption is limited by the formate decomposition temperature. Only a very small amount of CO_2 is detected. Therefore formic acid decomposes predominantly in a dehydration reaction on the YSZ surface.

Desorption spectra on a thin film of ZrO_2 grown on YSZ are shown in Figure 6. The as-grown sample shows desorption of both CO and CO_2 at ~590 K. The peaks are not very pronounced (see Figure 6a). The CO_2 desorption peak is somewhat more pronounced than the CO peak. Annealing the film in 10^{-6} Torr O_2, and only flashing the sample very briefly to 700 K in UHV increases the CO_2 desorption peak at the expense of the CO peak (see Figure 6b). After sputtering and annealing, the peak areas for CO and CO_2 increase strongly; this is shown in Figure 6c. The peak intensity is about the same for CO and CO_2, indicating that both dehydration and dehydrogenation reactions occur with about equal probability. Annealing the thin ZrO_2 film ex situ in a tube furnace in atmospheric pressure O_2, which reduces the step-edge density, and then returning it to the TPD chamber completely quenches any formic acid adsorption, and no CO or CO_2 desorption signals are observed. This is evident from Figure 6d.

Finally we also studied a pure 2−3 nm thick Y_2O_3 film grown on a YSZ(111) substrate. The TPD spectra are shown in Figure 7. The as-grown film exhibits a strong CO desorption peak and

TABLE 1: TPD Peak Intensities for CO and CO_2 of Different Samples and Preparation Procedures

	ZrO_2			YSZ		Y_2O_3	
products	as grown	O_2 annealed in UHV	sputtered and annealed	sputtered and annealed	O_2 annealed in furnace	as grown	O_2 annealed in furnace
CO	7.9	5.9	35.5	57.8	6.2	113.0	13.0
CO_2	13.0	16.2	28.6	0	0	6.1	3.2

only a weak CO_2 desorption feature at 600 K. The CO peak is more intense than for the other samples. Sputtering and annealing of the sample causes a further suppression of the already weak CO_2 peak without significant change in the CO desorption signal (not shown). Annealing of the sample in a tube furnace causes a reduction in the CO desorption intensity. However, unlike YSZ and ZrO_2, a clear desorption signal can still be discerned at ~600K.

4. Discussion

The TPD peak intensities for CO and CO_2 for the different samples are summarized in Table 1. Clearly, only pure ZrO_2 samples show a significant dehydrogenation reaction under the experimental conditions. The strong differences between YSZ and ZrO_2 indicate that the addition of yttrium to zirconia affects its chemical functionality to the extent that the reaction of formate on the YSZ(111) surface has stronger similarities to pure yttria than zirconia. This suggests that the active sites on YSZ surfaces are yttria-like. This is likely explained by the experimental observation of yttria segregation to the surface. The correlation between step densities observed in STM and chemical reactivity for formate adsorption indicates that step edges are of particular importance for describing the chemical reaction of formate on the surfaces considered. The importance of undercoordinated sites, such as step edges, in chemical transformation reactions on metal oxides is well-known.[28] Our observations that formate only adsorbs on a highly stepped YSZ(111) surface at room temperature illustrates the importance of such sites. Therefore, additives to an oxide ceramic may affect the surface chemical properties strongly if it preferentially segregates to these active sites. Segregation of 'impurities' to lower coordinated sites can reduce the system's energy by reducing lattice strain due to ion-radii mismatch between host and impurity cations, or by enabling adoption of lower preferred coordination numbers of the impurity at step edges. Y^{3+} has a 18% larger ionic radius than Zr^{4+}, and the coordination number for cations in Y_2O_3 is 7 compared to 8 in cubic ZrO_2. These effects may explain the computational results indicating that the step edges are preferentially yttria terminated.

Whereas formate decomposes in a dehydration as well as in a dehydrogenation reaction at steps of pure ZrO_2 under the vacuum conditions of the experiments, formate decomposes in a mainly dehydration reaction if yttria is added to zirconia. This shift in the selectivity is consistent with the preferential segregation of yttria to active surface sites and thus explains why the YSZ surface shows similar activity to pure Y_2O_3, which also mainly promotes dehydration reactions of formate.

Although we have not directly measured the role of lattice oxygen in the reaction, by, for example, isotopic labeling, it is known that lattice oxygen is actively involved in dehydrogenation reactions of formate.[10] Consequently, we speculate that the change in the selectivity between pure ZrO_2 and YSZ may be related to the availability of extractable lattice oxygen at the active step edge sites. The lower oxygen coordination number in yttria compared to zirconia suggests a lower O concentration at yttria-terminated step edges compared to a zirconia step edge. Consequently, formate adsorbed at step edges has less lattice oxygen to interact with on YSZ surfaces than on pure ZrO_2 and thus may explain the observed suppression of dehydration reactions under vacuum conditions. It is worth pointing out that a preference for dehydration reactions under vacuum conditions compared to high pressure studies is commonly observed on oxide surfaces,[10] and therefore our conclusions for YSZ surfaces may not hold in more oxidizing environments where step edge anion sites may become occupied by more easily extractable oxygen ions, and thus dehydrogenation reactions may become possible on the YSZ surface.

For pure ZrO_2, both dehydration and dehydrogenation reactions are observed in vacuum. This implies that step edges of zirconia are more readily reducible than yttria step edges and thus enable dehydrogenation reactions. Although zirconia is not commonly considered a reducible oxide, there is some evidence that it can be partially reduced by, e.g., CO.[29,30] Therefore our proposed reaction mechanism that involves lattice oxygen by scrambling oxygen from the surface with oxygen in the molecules seems plausible. In such processes, oxygen is interchanged between the molecules and the oxide lattice and thus the overall oxygen concentration at the surface remains unchanged, i.e., no reduction of the surface occurs.

5. Conclusion

An interplay between experimental surface science characterization of YSZ and advanced computational methods enabled determination of the importance of yttria addition to zirconia for the surface chemical properties. Yttria segregation modifies step edges and thus strongly alters the active sites in YSZ. The modification of active sites in mixed oxide ceramics by the minority component is likely to be active in many other ceramics and needs to be assessed in order to fundamentally understand their functionalities.

Acknowledgment. This material is based upon work supported by the National Science Foundation under CHE-0840547. The authors gratefully acknowledge the allocation of time and services in the Scienta ESCA Laboratory of Lehigh University and the professional and technical assistance of Dr. Alfred C. Miller.

References and Notes

(1) Buban, J. B.; Matsunaga, K.; Chen, J.; Shibata, N.; Ching, W. Y.; Yamamoto, T.; Ikuhara, Y. *Science* **2006**, *311*, 212.
(2) Nernst, W. *Z. Elektrochem.* **1899**, *6*, 41.
(3) Chen, L. B. *Surf. Rev. Lett.* **2006**, *13*, 535.
(4) Zhu, J.; van Ommen, J. G.; Lefferts, L *J. Catal.* **2004**, *225*, 388.
(5) Zhu, J.; van Ommen, J. G.; Knoester, A.; Lefferts, L *J. Catal.* **2005**, *230*, 291.
(6) Barteau, M. A. *Chem. Rev.* **1996**, *96*, 1413.
(7) Peng, X. D.; Barteau, M. A. *Catal. Lett.* **1990**, *7*, 395.
(8) Lintuluoto, M.; Nakatsuji, H.; Hada, M.; Kanai, H. *Surf. Sci.* **1999**, *429*, 133.
(9) Stubenrauch, J.; Brosha, E.; Vohs, J. M. *Catal. Today* **1996**, *28*, 431.
(10) Fein, D. E.; Wachs, I. E. *J. Catal.* **2002**, *210*, 241.
(11) Kim, K. S.; Barteau, M. A. *Langmuir* **1990**, *6*, 1485.
(12) Majumdar, D.; Chatterjee, D. *J. Appl. Phys.* **1991**, *70*, 988.

(13) Bernasik, A.; Kowalski, K.; Sadowski, A. *J. Phys. Chem. Solids.* **2002**, *63*, 233.
(14) Wang, X.-G. *Surf. Sci.* **2008**, *602*, L5.
(15) Xia, X.; Oldman, R.; Catlow, R. *Chem. Mater.* **2009**, *21*, 3576.
(16) Nowotny, J. *Solid State Ionics* **1991**, *49*, 119.
(17) Zhu, J.; Albertsma, S.; van Ommen, J. G.; Lefferts, L. *J. Phys. Chem. B* **2005**, *109*, 9550.
(18) Kim, Y. J.; Thevuthasan, S.; Shutthananadan, V.; Perkins, C. L.; McCready, D. E.; Herman, G. S.; Gao, Y.; Tran, T. T.; Chambers SA, S. A.; Peden, C. H. F. *J. Electron Spectrosc. Relat. Phenom.* **2002**, *126*, 177.
(19) Morrow, S. L.; Luttrell, T.; Carter, A.; Batzill, M. *Surf. Sci.* **2009**, *603*, L78.
(20) Green, R. G.; Barre, L.; Giorgi, J. B. *Surf. Sci.* **2007**, *601*, 792.
(21) Chenoweth, K.; van Duin, A. C. T.; Goddard, W. A., III. *Angew. Chem., Int. Ed.* **2009**, *48*, 7630.
(22) Mayernick, A. D. Batzill, M. Janik, M. J. van Duin, A. C. T. To be published.
(23) Seah, M. P.; Dench, W. A. *Surf. Interface Anal.* **1979**, *1*, 2.
(24) Briggs D., Seah M. P. *Practical Surface Analysis*; John Wiley & Sons: Chichester, 1983; Vol. 1, ISBN0-471-92081-9.
(25) Henderson, M. A. *J. Phys. Chem.* **1995**, *99*, 15232.
(26) Dilara, P. A.; Vohs, J. M. *J. Phys. Chem.* **1993**, *97*, 12919.
(27) Idriss, H.; Lusvardi, V. S.; Barteau, M. A. *Surf. Sci.* **1996**, *348*, 39.
(28) Thomas, J. M. *Top. Catal.* **2008**, *50*, 98.
(29) Stagg, S. M.; Romeo, E.; Padro, C.; Resasco, D. E. *J. Catal.* **1998**, *178*, 137.
(30) Sharma, S.; Hilaire, S.; Vohs, J. M.; Gorte, R. J.; Jen, H. W. *J. Catal.* **2000**, *190*, 199.

JP9109964